

# Indirect Vector Control of a Redundant Linear Induction Motor for Aircraft Launch

David C. Meeker, *Member, IEEE* and Michael J. Newman, *Member, IEEE*

**Abstract**—The potential for high force and low inertia makes the long stator linear induction motor a good candidate for use in aircraft launch. These motors typically have a segmented stator which runs the entire length of travel. A conductive plate is used as the moving shuttle. If high reliability is desired, one approach is to drive shuttle plate using multiple, separately excited stators. Although the stators are separately excited, the stators are still coupled via mutual inductance and common current paths in the shuttle plate. This paper considers the development of an indirect vector control scheme that accommodates the cross-coupling between stators and allows responsive control of the total force on the shuttle in the presence of faulted stators.

**Index Terms**—Electromagnetic launching, Linear induction motors, Motor drives, Fault tolerance

## I. INTRODUCTION

The electromagnetic catapults designed for U. S. Navy's Electromagnetic Aircraft Launch System (EMALS) program are predominately driven by three requirements (approximately captured in [1] and [2]):

1. Produce a sustained launch force of  $\sim 1.3$  MN
2. Achieve launch speeds of up to  $\sim 100$  m/s (over a stroke of  $\sim 100$  m)
3. Brake the shuttle (with the launch motor) after aircraft release over a stroke of less than 10 m.

The simultaneous realization of these performance requirements leads to the development of an unusual motor topology for EMALS that required the development of a novel control approach. To motivate the discussion of this control approach, some of the design drivers that lead to the current motor design and control scheme will be discussed.

### A. Selection of linear motor topology

Both Linear Permanent Magnet Synchronous Motors (LPMSMs) and Linear Induction Motors (LIMs) have been

considered for use as aircraft catapults. All modern designs are so-called “long-stator” machines, where a wound, segmented stator runs the entire length of travel. The moving shuttle consists of an array of permanent magnets for LPMSMs or an electrically conductive plate in the case of LIMs. These motors typically have a double-sided topology, *i.e.* a stator is located on either side of the shuttle.

Both LPMSMs and LIMs are capable of producing large forces. However, the selection of linear motor type must also consider the maximum speed and shuttle braking requirements.

LPMSM designs that realize high force with low weight shuttles have a fairly short pole pitch [3]. At a  $\sim 100$  m/s launch speed, typical LPMSM designs have a fundamental frequency in the range 300-700 Hz [1]-[4]. To drive a brushless DC motor, at least six switching events must occur per electrical cycle, implying that the switching frequency of the drive electronics must be, at a minimum, in the range of 1800-4200 Hz. High-force LIMs, however, favor longer pole pitch designs that with fundamental frequencies in the range of 50-150 Hz [3][5]. High-power drives based on today's IGBT or IGCT technologies switch at frequencies in the 1's of kHz. LPMSMs that can produce high-end launch speeds border the limits of the capabilities of today's drives, whereas the frequencies required by the LIMs are a well within the range of existing technology.

The requirement to brake the shuttle in a short distance after launch also drives the selection of a LIM. An aluminum plate shuttle is light relative to the permanent magnet shuttle required to obtain the same thrust. A reduction by a factor of four in shuttle weight for LIMs relative to LPMSMs is predicted in [3].

Because LIMs are currently a better match to available power electronics and to the shuttle braking requirements of the EMALS system, a long-stator LIM is considered for the purposes of the present work. Indeed, both launch motors constructed during the competitive Program Definition and Risk Reduction (PDRR) phase of the U. S. Navy's Electromagnetic Aircraft Launch System (EMALS) program were LIMs.

### B. Selection of control methodology

Several performance attributes of the system guide the selection of a control methodology:

- *Transient response.* The transient response requirements of the motor are dominated by the requirement to brake the shuttle after launch. The

Manuscript received July 3, 2008.

D. C. Meeker is with Foster-Miller Inc., 350 Second Ave., Waltham, MA 02154, USA (phone: 781-684-4070; fax: 781-890-3489; e-mail: [dmeeker@ieee.org](mailto:dmeeker@ieee.org)).

M. J. Newman is with the Electromagnetic Systems division of General Atomics, 16969 Mesamint Street, San Diego, CA 92127, USA (email: [ieee@michael-newman.com](mailto:ieee@michael-newman.com))

NAVAIR Public Release 08-642; Distribution: Statement A – “Approved for public release; distribution is unlimited”

controller must be able to slew the motor force from full launch force to full braking force over a very short duration and then apply a constant braking force over the remainder of the braking event.

- *Low-speed performance.* The system must provide well-regulated control over a speed range that includes zero speed.
- *Positioning.* The system must accommodate hard positioning requirements, *i.e.* launch speed achieved at a particular point on deck and a  $\sim 10$  m braking run-out.

An approach with the capability to satisfy all of these requirements is vector control with position sensing.

A redundant encoder system is used to provide position both for the purposes of the vector control algorithm and for position feedback control of the launch profile. To simplify the controller as much as possible, a feed-forward indirect vector control [6] approach is adopted. Per this approach, the desired slip frequency is computed based on the commanded magnetizing currents and commanded motor force.

Although driven by the requirement to brake the shuttle, the selection of a vector control paradigm also provides other advantages to the EMALS system:

- Closed-loop tracking of a desired shuttle position profile during launch results in a well-regulated holdback release, low peak accelerations, and the tight control of launch speed in the presence of uncertainties.
- High bandwidth closed-loop current control associated with a vector control implementation masks the effects of motor impedance variations (*i.e.* current spikes and disturbance force) during transitions between motor segments.
- The same closed-loop position-tracking controller structure can be used to retract and/or precisely position the shuttle between launches.

### C. Fault Tolerant Operation

Since EMALS is a man-rated system, the Navy has specified stringent reliability requirements. To meet these requirements, it was necessary to build fault tolerance into the design of the motor and controller. Two methods that have been considered in the literature include:

- Independent control of each phase in a three-phase stator [1]
- Use of multiple, independent stators driving a single shuttle [4]

A redundant stator approach was adopted here because failure scenarios are feasible in which multiple phases could be taken down by a single failure, *e.g.* phase-to-phase short. In a redundant stator approach, if any sort of error is detected, the offending stator can be turned off, and the launch can be completed using the remaining stators.

Although redundant stators have been considered in the literature, previous work only considered this approach as

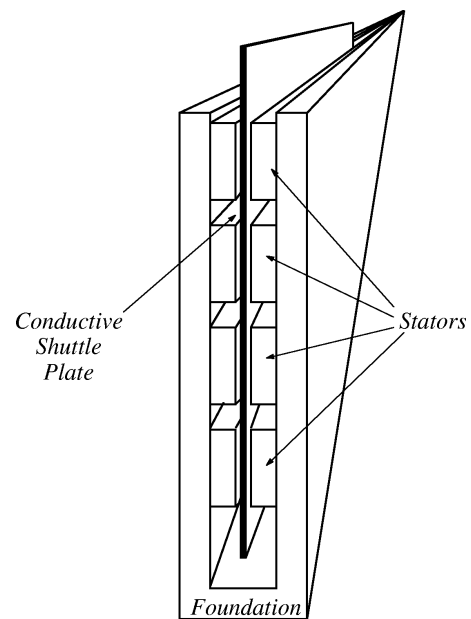


Fig. 1. Cross-section of a redundant double-sided long-stator linear induction motor.

applied to LPMSMs. For this sort of machine, multiple stator vector control is straightforward—the motors are essentially electrically identical and uncoupled. Each motor can be controlled using a straightforward synchronous motor vector control approach with each stator sharing an equal portion of the total force. For LIMs, the situation is very different. The straightforward approach to designing a LIM with redundant stators is to stack the stators on top of one another with all stators acting upon the same conductive plate, as shown in Figure 1. In this design, however, the stators are *not* independent—common current flow paths in the shuttle plate couple the stators together in a significant way.

The presence of common current flow paths has interesting ramifications. Firstly, all stators must be controlled so that the slip frequency is exactly the same from stator to stator. If the electrical frequencies of adjacent stators are different, the common current flow paths will result in disturbance forces at the beat frequency of the stators. Second, the common current flow paths influence the orientation and magnitude of the flux in the adjacent stators. To control a redundant-stator linear induction motor, a generalized version of indirect vector control is required that accommodates the cross-couplings between stators due to common current flow paths and stator-to-stator mutual inductances.

### D. Objectives

A generalized indirect vector control formulation that allows for multiple, coupled stators does not exist in the literature. The present work derives a novel form of indirect vector control that accommodates the cross-coupling between stators and allows for independent control of flux in each stator and total motor force. Since the purpose of the multiple stator geometry is fault-tolerance, several methods for tolerating a failed stator are presented. Finally, the experimental performance of one of the fault-tolerance methods on a full-scale linear induction catapult is considered.

## II. MOTOR MODEL

One desirable attribute of the long-stator LIM configuration is that longitudinal end effects are largely negligible for the purposes of control if the shuttle is several wavelengths long[5]. In contrast, longitudinal end effects are a strong effect that must be directly accommodated in the vector control of short-stator LIMs [7]. If end effects are neglected, the simple motor model pictured in Figure 2 can be used for the purpose of motor control. The equivalent circuit in Figure 2 has the same structure as the equivalent circuit of a typical induction machine that has been arranged so that all of the leakage appears lumped together on the stator side of the circuit. Unlike the single-stator case, however, currents  $i_s$ ,  $i_d$ , and  $i_q$  are vectors of stator, magnetizing, and shuttle current, respectively, containing  $n$  entries (one for each of  $n$  stators). Instead of scalar values,  $R_s$ ,  $R_r$ ,  $L_l$ , and  $M$ , representing stator resistance, shuttle resistance, leakage inductance, and mutual inductance respectively, are positive definite  $n \times n$  matrices. The couplings between the stators are characterized by the off-diagonal elements in the various resistance and inductance matrices.

The complex-valued currents pictured in Figure 2 are related to the phase currents via the transformation:

$$i_{s,n} = j\sqrt{\frac{2}{3}}e^{-j\theta} \left\{ 1, -\frac{1}{2} - j\frac{\sqrt{3}}{2}, -\frac{1}{2} + j\frac{\sqrt{3}}{2} \right\} \begin{Bmatrix} i_{a,n} \\ i_{b,n} \\ i_{c,n} \end{Bmatrix} \quad (1)$$

and the reverse transformation:

$$\begin{Bmatrix} i_{a,n} \\ i_{b,n} \\ i_{c,n} \end{Bmatrix} = \text{Re} \left[ -j\sqrt{\frac{2}{3}}e^{j\theta} \begin{Bmatrix} 1 \\ -\frac{1}{2} + j\frac{\sqrt{3}}{2} \\ -\frac{1}{2} - j\frac{\sqrt{3}}{2} \end{Bmatrix} i_{s,n} \right] \quad (2)$$

where  $i_{s,n}$  and  $i_{abc,n}$  represent the complex space vector version of stator current and phase currents for the  $n^{\text{th}}$  stator respectively. For a detailed discussion of the complex space vector representation of three-phase currents, refer to [8].

## III. DERIVATION OF MULTISTATOR INDIRECT VECTOR CONTROL

As in ordinary indirect vector control, the goal is to obtain an expression for the commanded current that consists of a constant magnetizing component plus a force-producing component that varies linearly with the desired motor force. For the purposes of deriving a generalized version of vector control, it will be assumed that all stators are current-controlled, such that the steady-state circuit pictured in Figure 2 can be simplified to the current-controlled motor equivalent circuit pictured in Figure 3. Since each stator is current controlled, all stator impedances can be neglected (at least for the purposes of developing the vector control algorithm).

### A. Shuttle current in terms of magnetizing current and slip

The first step in deriving the vector control algorithm is representing shuttle current  $i_q$  in terms of magnetizing current

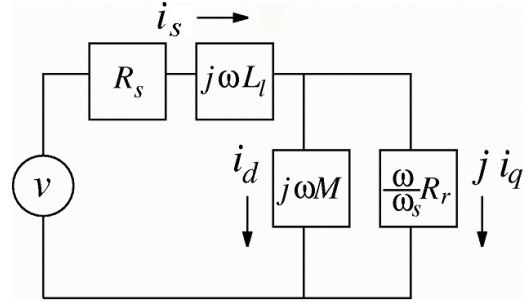


Fig. 2. Circuit diagram of steady-state four-stator motor model.

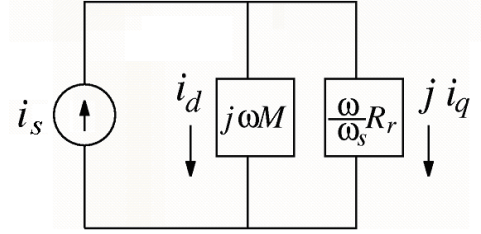


Fig. 3. Motor model assuming stiff current control.

$i_d$ . Evaluating the voltage loop equation around the shuttle branch of the circuit yields:

$$j\omega M i_d = j\frac{\omega}{\omega_s} R_r i_q \quad (3)$$

which can be solved for  $i_q$  to yield:

$$i_q = \omega_s R_r^{-1} M i_d \quad (4)$$

Knowing the shuttle current, an expression for the total current can be written as:

$$i_s = i_d + j i_q = i_d + j\omega_s R_r^{-1} M i_d \quad (5)$$

Equation (5) is important because it allows the controller to pick an arbitrary value of magnetizing current,  $i_d$ , and then command stator currents that maintain a constant flux linking the shuttle regardless of the slip frequency. The slip frequency can then be selected so that the desired motor force is obtained.

### B. Slip frequency as a function of motor force

Ultimately, the goal is to select the currents to obtain some particular desired force. To do this, a relationship between slip frequency  $\omega_s$  and force  $F$  is required. The first step is to obtain a relationship for motor force. To obtain an expression for motor force, the power dissipated in the shuttle can be evaluated:

$$P = \frac{\omega}{\omega_s} i_q^* R_r i_q \quad (6)$$

where the asterisk superscript denotes the transpose of the complex conjugate of a vector or matrix.

The shuttle power is composed of two parts: resistive power losses in the shuttle, and mechanical power applied to the load. The resistive power losses are:

$$P_{resistive} = i_q^* R_r i_q \quad (7)$$

Subtracting this power from the total power yields the mechanical power:

$$P_{mech} = \frac{\omega - \omega_s}{\omega} i_q^* R_r i_q \quad (8)$$

To obtain mechanical force, it can be noted that mechanical power is the product of force and velocity. It can also be noted that the  $\omega - \omega_s$  quantity is the mechanical frequency of the system, which we can define as being equal to  $k v$ , the velocity of the shuttle times the wavenumber,  $k$ , that converts length to electrical angle. Wavenumber is defined as:

$$k = \frac{\pi}{\text{Pole Pitch}} \quad (9)$$

The resulting motor force is:

$$F = \frac{k}{\omega_s} i_q^* R_r i_q \quad (10)$$

However, since the vector control scheme regulates magnetizing current  $i_d$  rather than shuttle current, it is desirable to write the force expression in terms of magnetizing current, rather than in terms of shuttle current. This can be done by applying the previously derived relationship between shuttle currents (4) to yield:

$$F = k \omega_s i_d^* M R_r^{-1} M i_d \quad (11)$$

When written in this form (*i.e.* when the magnetizing currents are specified), there is a linear relationship between slip frequency and force. The slip frequency required to obtain any particular force is then:

$$\omega_s = \frac{F}{k i_d^* M R_r^{-1} M i_d} \quad (12)$$

### C. Indirect vector control scheme

If it is assumed that  $i_d$  is held constant, the above derivations immediately lead to an indirect vector control algorithm:

$$\begin{aligned} i_d & \text{ is selected "arbitrarily"} \\ \omega_s & = \frac{F}{k i_d^* M R_r^{-1} M i_d} \\ i_q & = \omega_s R_r^{-1} M i_d \\ i_s & = i_d + j i_q \end{aligned} \quad (13)$$

Assuming that the shuttle position,  $x$  is measured, the electrical angle used to convert these currents back into actual phase currents is then obtained by:

$$\theta = k x + \int \omega_s dt \quad (14)$$

The above three equations are used to convert a desired force command into a set of instantaneous current commands that realize the desired force.

### D. Accommodation of varying magnetization current

The above algorithm assumes that  $i_d$  is constant. If  $i_d$  is changed on-the-fly, the field linking the shuttle does not change instantaneously. Consequently, the  $i_q$  currents must be chosen in a slightly different fashion to account for the instantaneous flux in the gap. In particular, a net magnetization current,  $i_n$  can be defined that is, in the steady-state, the same as  $i_d$ , but settles in based on the electrical dynamics of the shuttle:

$$\frac{di_n}{dt} = M^{-1} R_r (i_d - i_n) \quad (15)$$

The  $i_q$  current is then selected based on the net magnetizing current, rather than the  $i_d$  current:

$$\begin{aligned} i_q & = \omega_s R_r^{-1} M i_n \\ \omega_s & = \frac{F}{k i_n^* M R_r^{-1} M i_n} \end{aligned} \quad (16)$$

## IV. ACCOMMODATION OF FAULTS

The purpose of the multiple-stator geometry is the fault-tolerant operation. It is assumed that there is a centralized controller that is implementing the vector control algorithm and selecting currents for all stators. If a stator fails, the controller must respond in a way that accommodates the failure. Three approaches for tolerating stator failures within the indirect vector control paradigm are discussed in the subsequent sections.

### A. Approximate accommodation of stator-out

Perhaps the simplest possible way of tolerating a failed stator is to replace the commanded  $i_d$  in the failed stator with zero, and then proceeding as normal. Replacing the  $i_d$  with zero has the effect of requiring no force from the failed stator. It can be noted that since the commanded  $i_q$  is produced by (4), which has couplings from stator to stator, the commanded  $i_q$  in the failed stator can be non-zero, even if the commanded  $i_d$  is zero. Although the  $i_q$  command in the failed stator cannot be realized if the stator is failed, the commanded  $i_q$  is typically small in magnitude (since the non-zero  $i_q$  is driven by the couplings between stators). Since this scheme does not exactly invert the electrical dynamics of the shuttle, some dynamics are added back in to the relationship between commanded and actual force.

### B. Accommodation via isolation of failed stator

One important feature of the generalized indirect vector control strategy is that all magnetizing ( $i_d$ ) currents can be chosen essentially arbitrarily (at least, in isolation of the force which is being produced). A way to accommodate a stator-out is to consider the stator-out as merely being constraints on the selection of the  $i_d$ 's.

The first, and most obvious, constraint would be that the component of  $i_d$  associated with the failed stator must be zero. Since the current,  $i_s$ , required from the stators is the combination of  $i_d$  and  $i_q$ , the total current required from the failed stator can be set to zero by choosing the remaining  $i_d$  currents so that the required  $i_q$  in the failed stator is always zero. Recalling (4), the relationship between  $i_d$  and  $i_q$ , the two constraints on the selection of the  $i_d$ 's that guarantee a zero net current for the failed stator are:

$$\begin{aligned} pR_r^{-1}Mi_d &= 0 \\ pi_d &= 0 \end{aligned} \quad (17)$$

where  $p$  is a vector that has all zero entries except for a one in the location corresponding to the failed stator. For example, if the third stator were failed,  $p$  would be:

$$p = \{0, 0, 1, 0\} \quad (18)$$

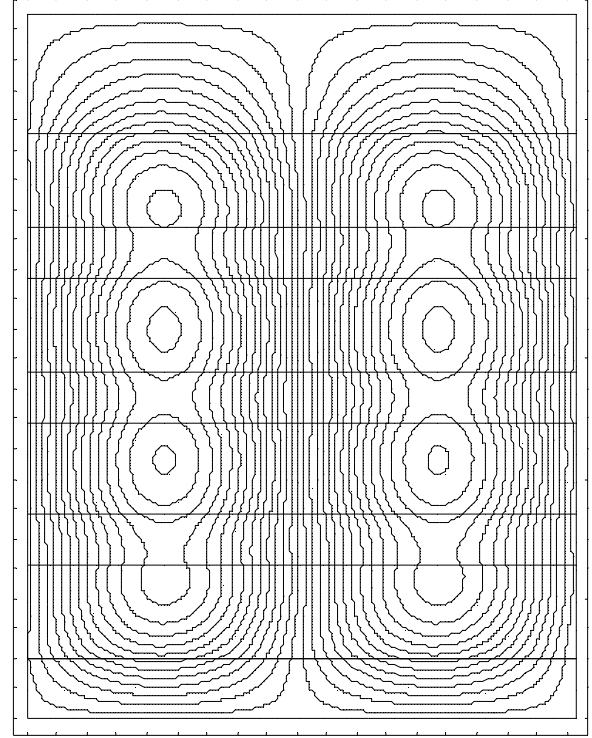
One is then free to arbitrarily choose any two of the  $i_d$ 's for the non-failed stators, with the other two  $i_d$ 's being prescribed by the linear constraints.

This strategy produces  $i_d=i_q=0$  for the failed stator regardless of what force is being produced. This strategy changes the current flow paths so that nominally, no flux links the failed stator, making the strategy suitable for either failed-open or failed-short instances. An illustration of the different current flow patterns in the shuttle in the nominal and failed cases is shown by the 2D finite element solutions for plate currents in Figure 4.

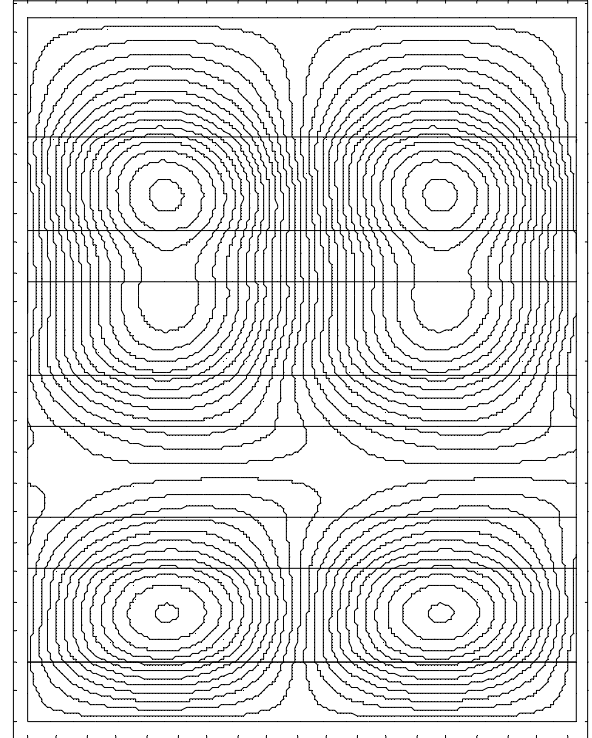
Although this strategy handles the failed stator in a robust way, this strategy has some undesirable properties when implemented in simulation. To isolate the failed stator, the  $i_d$ 's of the stators on either side of the failed stator must be of opposite sign. Nominally, all of the  $i_d$ 's have the same sign and similar amplitudes (*i.e.* so that the lowest shuttle losses can be realized under nominal operating conditions). The result is that there is a fairly long-duration transient between the nominal and failed  $i_d$  mappings, during which the motor does not perform very well (*i.e.* requests high current to get the required force).

### C. Accommodation via direct current variation

The "isolation method" requires both the  $i_d$  and  $i_q$  components for a failed stator to be zero, so that the total current (which is the sum of  $i_d$  and  $i_q$ ) will always be zero. A less restrictive method of rigorously tolerating stator-out is to simply enforce zero sum of  $i_d$  and  $i_q$  in the failed stator, *i.e.* the instantaneous  $i_d$  for the failed stator is chosen so that the sum of the currents in the failed stator is equal to zero:



Nominal Current Distribution



Current Distribution with isolated third stator

Fig. 4. Shuttle current flow paths in nominal and failed cases.

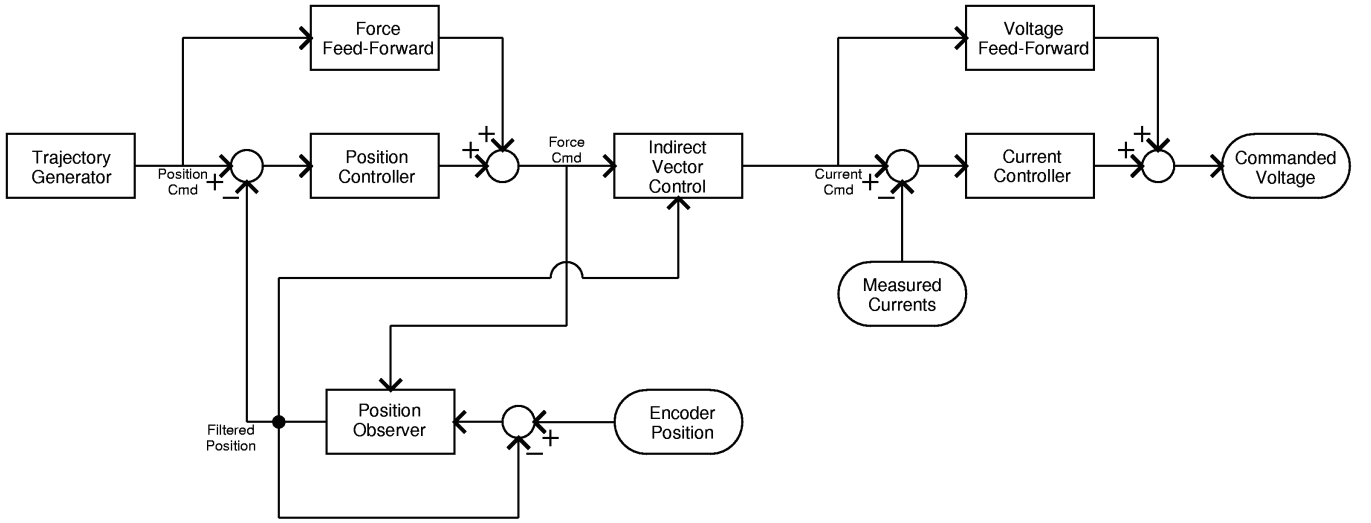


Fig. 5. Controller block diagram.

$$i_{d,n}(t) = -ji_{q,n}(t) \quad (19)$$

where the  $n$  subscript is meant to denote the  $n^{\text{th}}$  failed stator. The varying  $i_d$  formulation described in (16) is then used to accommodate the varying  $i_d$  of the failed stator.

However, note that this algorithm forces both  $i_d$  and  $i_q$  to be complex valued. With other schemes, if  $i_d$  is selected to be real-valued, the resulting  $i_q$  is real-valued, simplifying the real-time calculations that must be done to support. The requirement of complex-valued calculations increases the amount of time required to perform the vector control calculations by approximately a factor of 4.

## V. EXPERIMENTAL RESULTS

The four-stator vector control algorithm with approximate accommodation of stator-out failures was implemented on the Electromagnetic Aircraft Launch System (EMALS) Program Definition and Risk Reduction (PDRR) machine built by General Atomics and located at Naval Air Engineering Station (NAES) Lakehurst [9]. The EMALS PDRR machine has a full-scale cross-section and shuttle, but only half the length of the planned shipboard machine.

The machine is segmented into 13 motor blocks, each 12 ft long. The shuttle spans two blocks. So that the shuttle is always contained within an active section of stator, three stator blocks are turned on at all times. The IGBT-based power system can apply a peak phase voltage of 4kV and support a peak phase current of 18kA. Each stator has its own electrically independent inverter system. Each stator has a dedicated flywheel and generator that supply power to the stator's inverter system.

In addition to the indirect vector control algorithm described in this paper, the controller also implements a trajectory tracking control loop and a trajectory generator. The overall structure of the controller is shown in Figure 5. The controller structure is conceptually similar to the closed-

loop vector control implementation described in more detail in [5].

For the purposes of control, the following parameters are employed by the controller:

$$M = \begin{bmatrix} 514.8 & 48.0 & 11.8 & 4.9 \\ 48.0 & 492.0 & 51.2 & 11.9 \\ 11.8 & 51.2 & 499.0 & 48.8 \\ 48.8 & 11.9 & 48.8 & 477.5 \end{bmatrix} \mu H$$

$$R_r = \begin{bmatrix} 5.867 & -1.559 & -0.001 & -0.022 \\ -1.559 & 6.36961 & -1.421 & 0 \\ -0.001 & -1.421 & 6.505 & -1.578 \\ -0.022 & 0 & -1.578 & 6.853 \end{bmatrix} m\Omega$$

$$L_l = \begin{bmatrix} 500 & 0 & 0 & 0 \\ 0 & 500 & 0 & 0 \\ 0 & 0 & 500 & 0 \\ 0 & 0 & 0 & 500 \end{bmatrix} \mu H$$

$$R_s = \begin{bmatrix} 55 & 0 & 0 & 0 \\ 0 & 55 & 0 & 0 \\ 0 & 0 & 55 & 0 \\ 0 & 0 & 0 & 55 \end{bmatrix} m\Omega$$

$$k = 6.871 \text{ rad/m}$$

To test the ability to complete launches in the presence of a faulted stator, tests were performed using a deadload weighing 9,816 lb. The mass of the shuttle was 1800 lb. Two particular tests considered the acceleration of the deadload to a speed of 120 knots (61.73 m/s) over a 30 m launch stroke. The magnetizing currents selected for these launches were:

$$i_d = \begin{Bmatrix} 6525 \\ 6060 \\ 6163 \\ 7386 \end{Bmatrix} A$$

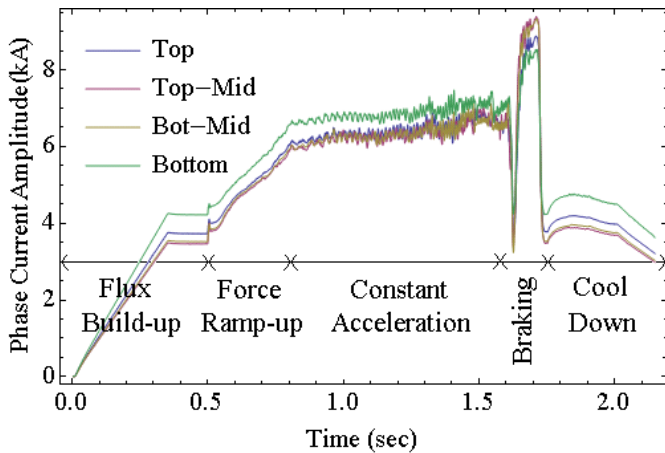


Fig. 6. Stator currents versus time for launch without faults.

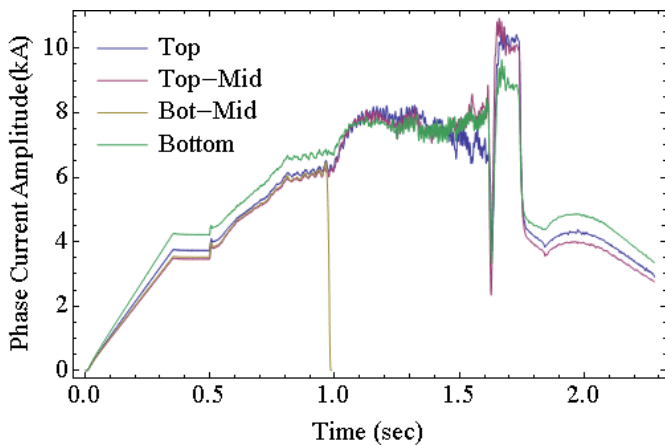


Fig. 7. Stator currents versus time for launch with a fault at ~1 sec.

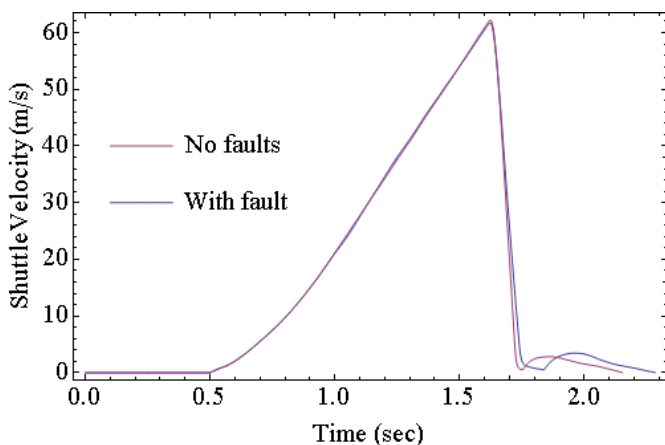


Fig. 8. Shuttle velocity versus time

The first test contained no failures. In the second test, a failure was seeded by disabling the block switches on the bottom-middle stator so that no current can flow to that stator at shuttle displacements greater than approximately 3 m down the track.

The phase currents for the fault-free launch are shown in Figure 6. The current amplitude is slightly different in each stator because slightly different magnetizing currents are

selected to balance the power delivered by each stator. The launch proceeds through five phases:

1. *Flux Build-up*. During the first half-second, the magnetizing currents are ramped up to establish a flux linking the shuttle.
2. *Force Ramp-up*. To reduce stress on the airframe, the controller tracks a launch profile that corresponds to a gradual ramp-up of force.
3. *Constant Acceleration*. The system tracks a trajectory corresponding to a constant acceleration.
4. *Braking*. Force rapidly slews from the force required for launch to a prescribed braking force. This braking force is maintained until the measured speed of the shuttle is less than a prescribed threshold.
5. *Cool Down*. Magnetizing currents are gradually ramped down.

Figure 7 shows the stator currents in the presence of a failure occurring at approximately one second into the launch. After that point, the currents are re-mapped assuming a zero magnetizing current for the failed stator. Higher currents on the remaining stators are required to make up for the contributions of the failed stator.

Figure 8 shows the measured velocity for each launch. A small response to the failure is visible on the curve for the launch in which a stator fails. However, both launches provide a launch velocity that is very close to the commanded end speed: 120.2 knots for the nominal launch and 119.9 knots for the launch with a failed stator. It should be noted that the shuttle brakes faster in the case of the nominal launch because higher braking forces were commanded for that launch. In both cases, the braking distance is less than the 20 ft. allocated for shuttle braking.

## VI. CONCLUSIONS

An indirect vector control algorithm has been derived for a long-stator linear induction motor in which multiple stators drive a single shuttle plate in parallel. The algorithm takes account of the significant stator-to-stator couplings that arise due to mutual inductance between stators and common current flow paths in the shuttle. Several methods of tolerating failed stators have also been presented. Of these methods, the simple approximate method (*i.e.* zero components of the  $i_d$  corresponding to failed stators and ignore  $i_q$  commanded on failed stator) has been tested on full-scale aircraft launch hardware, and this method provides an adequate recovery from stator-out in practice. Since the approximate method is simple and performs adequately, it appears to be the fault tolerant method of choice. Although this method only approximately inverts the shuttle's electrical dynamics, the method is computationally simple, and no change in  $i_d$  is required for the remaining healthy stators.

## REFERENCES

- [1] D. Patterson *et al.*, "Design and simulation of a electromagnetic aircraft launch system," *Proc. 37<sup>th</sup> Industry Applications Conference*, 2002.

- [2] M. R. Doyle, D. J. Samuel, T. Conway, and R. R. Klimowski, "Electromagnetic Aircraft Launch System – EMALS," *IEEE Trans. Mag.*, vol. 31, no. 1, pp. 528-533, Jan. 1995.
- [3] J. L. Kirtley, "On the linear synchronous/induction motor choice for electromagnetic aircraft launch," *Proc. ASNE Electric Machines Technology Symposium*, Philadelphia, PA, Jan. 2004.
- [4] G. Stumberger, D. Zarko, M. T. Aydemir, and T. A. Lipo, "Design and Comparison of Linear Synchronous Motor and Linear Induction Motor for Electromagnetic Aircraft Launch System," *Proc. IEEE International Electric Machines and Drives Conference (IEMDC 2003)*, Madison, WI, 2003.
- [5] A. P. Johnson, "High speed linear induction motor efficiency optimization," master's thesis, Dept. of Electrical Engineering and Computer Science, Massachusetts Institute of Technology, 2005.
- [6] B. K. Bose, *Modern Power Electronics and AC Drives*, Prentice-Hall, 2002.
- [7] S. C. Ahn, J. H. Lee, D. S. Hyun, "Dynamic characteristic analysis of LIM using coupled FEM and control algorithm," *IEEE Trans. Mag.*, vol. 36, no. 4, pp. 1876-1880, Jul. 2000.
- [8] D. W. Novotny and T. A. Lipo, *Vector Control and Dynamics of AC Drives*, Oxford University Press, 1996.
- [9] R. R. Bushway, "Electromagnetic aircraft launch system development considerations," *IEEE Trans. Mag.*, vol. 37, no. 1, pp. 52-54, Jan. 2001.